

# Self-starting simple structured dual-wavelength mode-locked erbium-doped fiber laser using a transmission-type semiconductor saturable absorber

Junkai Shi (石俊凯)<sup>1</sup> and Weihu Zhou (周维虎)<sup>1,2,\*</sup>

<sup>1</sup>Laboratory of Laser Measurement Technology, Academy of Opto-Electronics, Chinese Academy of Sciences, Beijing 100094, China

<sup>2</sup>University of Chinese Academy of Sciences, Beijing 100049, China

\*Corresponding author: zhouweihu@aoe.ac.cn

Received October 14, 2017; accepted January 12, 2018; posted online March 7, 2018

A self-starting simple structured dual-wavelength passively mode-locked (ML) erbium-doped fiber (EDF) laser is proposed in this Letter. An all-fiber ring cavity is adopted and a transmission-type semiconductor saturable absorber is used as modelocker. In this laser, there are two gain humps located at the 1530 nm region and the 1550 nm region, respectively. Along with the length of EDF increasing, the intensity of the hump at 1530 nm region is gradually suppressed because of the re-absorption of emission by the ground state. With the proper length of EDF, the gain intensities of two regions are very close. When the pump power is above the ML threshold, the self-starting dual-wavelength ML operation is achieved easily without manual adjustment. The two spectral peaks with close intensities are located at 1532 and 1552 nm, respectively. The effect of intracavity dispersion on the output spectrum is also experimentally demonstrated.

OCIS codes: 140.4050, 140.7090, 140.3510.

doi: 10.3788/COL201816.031404.

In recent years, multi-wavelength pulsed lasers have attracted great attention because of their versatile applications in optical signal processing, precision spectroscopy, biomedical research, microwave/terahertz photonics, and wavelength division multiplexed optical fiber communication systems<sup>[1-4]</sup>. A self-seeded or external injection seeded Fabry-Perot laser diode (LD)<sup>[5-9]</sup> was used to generate multi-wavelength pulses, which required a specially designed semiconductor laser cavity and external modulation. Multi-wavelength mode-locked (ML) pulses have also been achieved in solid lasers, such as a Ti:sapphire laser<sup>[10,11]</sup>, a neodymium-doped calcium niobium gallium garnet (Nd:CNGG) laser<sup>[12]</sup>, and a ytterbium-doped yttrium aluminum garnet (Yb:YAG) ceramic laser<sup>[13]</sup>. Comparatively, a ML fiber laser is an effective and simple way to generate multi-wavelength pulses. Several multi-wavelength actively ML fiber lasers have been reported. Schlager *et al.* demonstrated the dual-wavelength actively ML fiber ring laser based on a birefringent polarization maintaining fiber<sup>[14]</sup>. Multi-wavelength actively ML fiber lasers were also achieved by dispersive gratings<sup>[15]</sup>, a biased semiconductor optical amplifier<sup>[16]</sup>, a single sampled fiber Bragg grating<sup>[17]</sup>, or a highly nonlinear fiber<sup>[18]</sup> in the cavity. Pan *et al.* reported a multi-wavelength actively ML erbium-doped fiber (EDF) laser by virtue of the nonlinear polarization rotation (NPR) effect<sup>[19]</sup>. Jain *et al.* inserted an intensity modulator between the two polarization controllers (PCs), and multi-wavelength actively ML operation is achieved<sup>[20]</sup>.

Although multi-wavelength actively ML fiber lasers have the advantage of a high-repetition rate with a narrow line-width, multi-wavelength passively ML fiber lasers could be

preferred due to their intriguing advantages, such as ultra-short pulses, compactness, and low cost without a modulator required. Many multi-wavelength passively ML fiber lasers have been reported lately, and, in most cases, an all-fiber configuration is adopted because of great stability and low insertion loss. The NPR technique<sup>[21-24]</sup> and nonlinear optical loop mirror<sup>[25,26]</sup> have been utilized to achieve multi-wavelength ML operation in fiber ring cavities. Recently, the real saturable absorbers (SAs), such as the semiconductor SA mirrors<sup>[27,28]</sup>, single wall carbon nanotubes<sup>[29]</sup>, graphene<sup>[30]</sup>, and topological insulators<sup>[31,32]</sup>, have been used for multi-wavelength passive mode locking operation. In these aforementioned multi-wavelength passively ML all-fiber lasers, modulators, such as a PC<sup>[21-32]</sup> or loss attenuator<sup>[1,32]</sup>, were required in the cavity, which complicates the structure. In addition, multi-wavelength ML operation was achieved by adjusting the modulators to the proper state after laser working, which is inconvenient for use.

In this Letter, we experimentally demonstrate a self-starting simple structured dual-wavelength ML EDF laser by balancing intracavity gain and dispersion, which is similar to the work reported in Refs. [1,33] but with a much simpler cavity. A transmission-type semiconductor SA is used as mode locker in an all-fiber ring cavity. With the proper length of EDF in the cavity, the gain at the 1530 nm region is suppressed by emission re-absorption, and the gain intensities at both the 1530 nm region and 1550 nm region are very close. So, the self-starting dual-wavelength ML operation is achieved easily without manual adjustment. We also experimentally demonstrate the effect of intracavity dispersion on the output spectrum with fixed gain.

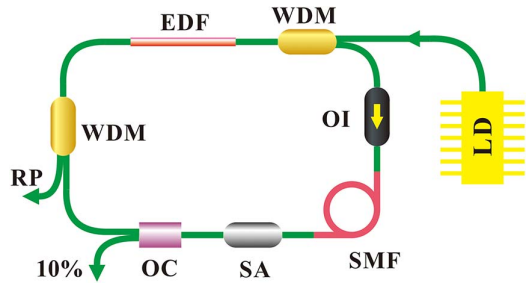


Fig. 1. Schematic of the experimental setup: LD, laser diode; WDM, wavelength division multiplexer; OC, optical coupler; SA, saturable absorber; EDF, Er-doped fiber; SMF, single mode fiber; OI, optical isolator; RP, residual pump.

The proposed dual-wavelength ML EDF laser scheme is shown in Fig. 1. The ring cavity is formed with a piece of 0.3 m EDF with an 8.8  $\mu\text{m}$  mode field diameter and a 55 dB/m core absorption at the 1530 nm wavelength. The group velocity dispersion (GVD) of the EDF is  $-0.016 \text{ ps}^2/\text{m}$ . Apart from the gain fiber, all of the other fibers are the standard single mode fiber (SMF) with a GVD of  $-0.022 \text{ ps}^2/\text{m}$ . A 976 nm LD delivering a maximum output power of 600 mW is used as a pump. The pump laser is introduced into the cavity through a standard single mode 976/1550 nm wavelength division multiplexer (WDM). The residual pump (RP) is coupled out of the cavity by another WDM. A polarization independent optical isolator (OI) is placed at the output of the backward-pumped EDF to ensure unidirectional operation of the light in the ring cavity. A fiber coupled Batop GmbH transmission-type semiconductor SA with a modulation depth, saturation fluence, and relaxation time of 35%, 300  $\mu\text{J}/\text{cm}^2$ , and 2 ps, respectively, is utilized to permit reliable self-starting ML operation. A 10:90 fiber optical coupler (OC) is employed to extract the output of the pulse, and 10% is used as the laser output. The length of the pigtail fibers is 3.24 m, and a piece of SMF after OI is used to change the intracavity dispersion. An optical spectrum analyzer (YOKOGAWA, AQ6370D), a digital storage oscilloscope (KEYSIGHT, DSO9254A), and a radio-frequency (RF) analyzer (KEYSIGHT, N9010A) together with a 1 GHz photodetector (PD) are employed to monitor the optical spectrum, the output pulse train, and the RF spectrum, respectively. Additionally, the pulse profile is measured by a commercial autocorrelator (APE PulseCheck).

Without additional SMF, the net intracavity dispersion is  $-0.0761 \text{ ps}^2$ , and self-starting dual-wavelength ML operation is achieved. The measured average output power versus pump power is shown in Fig. 2(a). The continuous wave (CW) output power increases monotonically from 0 to 0.53 mW as the pump power increased from 0 to 394 mW. The low conversion efficiency is attributed to small gain of a short EDF and large non-saturable loss of SA. With pump power slightly increased to 398 mW, the ML state is achieved, and the output power jumps

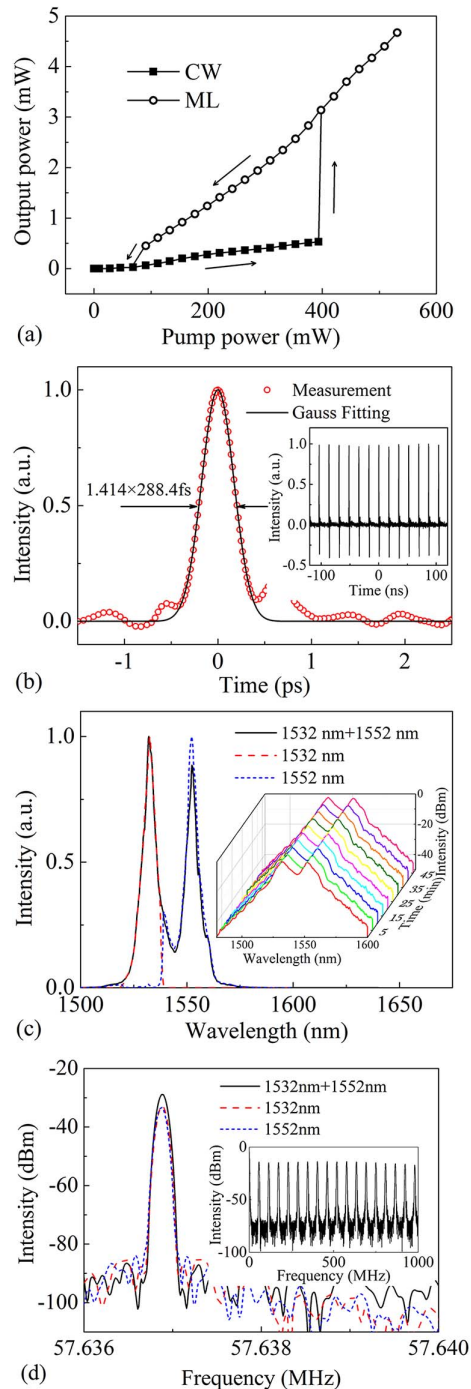


Fig. 2. ML output of the dual-wavelength oscillator at the pump power of 530 mW. Experimentally observed ML (a) output power and operating status of the laser vs. the pump power, (b) autocorrelation trace (inset: pulse train), (c) spectra of dual-wavelength and each single wavelength (inset: spectra measured at a 5 min interval over 45 min), and (d) RF spectra of dual-wavelength and each single wavelength (inset: RF spectrum measured in the 1 GHz range).

to 3.1 mW. The maximum ML output power of 4.7 mW is obtained when the pump power is 530 mW. In our experiment, the fiber laser can sustain the ML state when the pump power is decreased to  $\sim 90$  mW because of the pump hysteresis phenomenon<sup>[34]</sup>.

Figure 2(b) shows the autocorrelation trace. The autocorrelation function is 407.8 fs wide, thus corresponding to a pulse duration of 288.4 fs in the approximation of Gauss-shaped pulses. The corresponding pulse train is shown in the inset of Fig. 2(b). The period of the pulse train is about 17.35 ns, which matches with the cavity roundtrip time and verifies the ML state. The optical spectrum (black curve) under maximum pump power is measured at a 0.1 nm resolution and shown in Fig. 2(c). Apparently, there are two peaks at 1532 and 1552 nm with a 3 dB bandwidth of 6.2 and 5 nm, respectively, corresponding to a wavelength spacing of 20 nm. To verify the stability of the dual-wavelength ML fiber laser, the dual-wavelength pulse output is repeatedly scanned for 10 times with 5 min intervals, as shown in the inset of Fig. 2(c). There is no significant wavelength drift. Consequently, dual-wavelength ML pulses are verified with good stability at room temperature. The RF spectrum (black curve) is shown in Fig. 2(d). Its fundamental peak, located at the cavity repetition rate of 57.65 MHz, has a signal-to-noise ratio above 55 dB at a 10 Hz resolution bandwidth. The RF spectrum in a wider range (1 GHz) is shown in the inset of Fig. 2(d). The dual-wavelength pulse exhibits relatively good stability. Furthermore, we also provide optical spectra and RF spectra of each single wavelength using an extracavity bandpass filter, as shown in Figs. 2(c) and 2(d). The RF spectra of the dual-wavelength and each single wavelength show no obvious repetition rate difference, which, together with autocorrelation trace and pulse train, proves single pulse operation. Based on experimental results, we conclude that the fiber laser operates at a stable self-starting dual-wavelength ML state.

To reveal the reason for dual-wavelength operation, the dependence of the EDF length on the ML state is investigated. Figure 3(a) shows the dependence of the measured output amplified spontaneous emission (ASE) spectra on the length of EDF. The output ASE spectra are measured from the setup in Fig. 1 at low pump power without additional SMF. There are two humps located at the 1530 nm region and the 1550 nm region, respectively. When the length of EDF is 0.1 m, the hump of the ASE spectrum at the 1530 nm region is much higher than the one at the 1550 nm region. Along with the length of EDF increasing, the intensity of the hump at the 1530 nm region is gradually suppressed because of the typical characteristics of a three-level system, mainly the re-absorption of emission by the ground state<sup>[35]</sup>. When the length of EDF is 0.3 m, the intensities of the two humps are very close. By further increasing the EDF length, the intensity of the hump at a longer wavelength exceeds the one at a shorter wavelength, and the hump at the shorter wavelength almost vanishes when the EDF length is increased to 0.9 m. In addition, the hump at the 1550 nm region is moving toward the long wavelength with the length of EDF increased, while another hump at the 1530 nm region becomes weaker and weaker without the central wavelength shift.

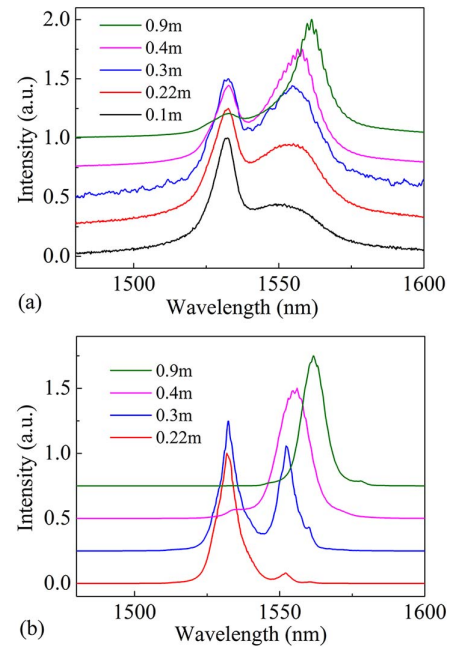


Fig. 3. (a) ASE spectra and (b) ML output spectra versus different lengths of EDF when the length of the SMF is fixed at 0 m.

The corresponding ML spectra with different length EDFs are shown in Fig. 3(b). The ML operation cannot be achieved with 0.1 m EDF because the gain is too low. When the EDF length is 0.22 m, the self-starting dual-wavelength ML operation is achieved. Because the gain at the 1530 nm region is much stronger than at the 1550 nm region, the ML spectrum at the 1550 nm region almost disappears, and the pulse energy is focused on the peak at the 1530 nm region. When the EDF length is 0.3 m, there are two spectral peaks with close intensities located at 1532 and 1552 nm, respectively, because the gain intensities of the two regions are very close. By further increasing the length of EDF, the pulse energy is focused on the peak at 1550 nm region. The spectral peak at the 1530 nm region is suppressed and eventually disappears. In addition, the spectral peak at the 1550 nm region red-shifts because the gain spectrum at the same region red-shifts.

The dependence of intracavity dispersion on the ML state is also experimentally investigated. Figure 4 shows the pulse trains and ML output spectra with different intracavity dispersions when the EDF length is fixed at 0.3 m. The ASE spectrum and output power are insensitive to the SMF length because of the EDF length being unchanged. Increasing the negative intracavity dispersion from  $-0.0761$  to  $-0.1324$  ps<sup>2</sup> by changing the SMF length from 0 to 2.56 m, the repetition rate is decreased from 57.65 to 33.46 MHz. The spectral peak at the 1550 nm region is strongly suppressed with the negative intracavity dispersion increased. This can be explained by the spectral compression effect induced by self-phase modulation with large negative intracavity dispersion<sup>[36]</sup>. The pulse energy is focused at the 1530 nm region, so the spectrum at the

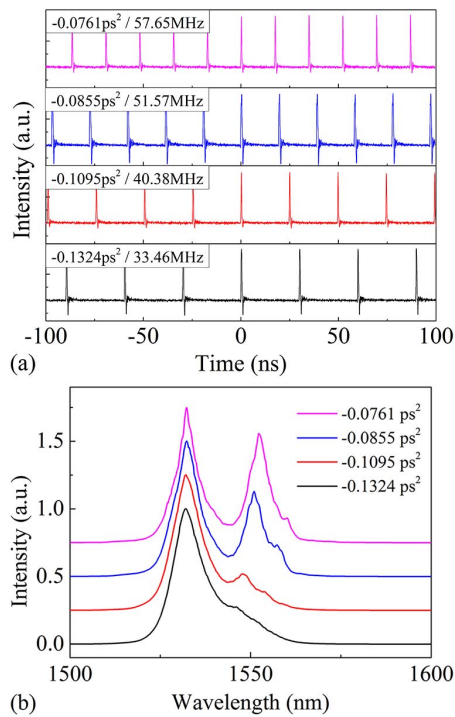


Fig. 4. (a) Pulse trains and (b) ML output spectra versus different intracavity dispersions when the EDF length is fixed at 0.3 m.

1530 nm region is slightly broadened. By balancing the intracavity gain and negative dispersion, dual-wavelength ML operation can be achieved.

In conclusion, we have experimentally investigated a self-starting simple structured dual-wavelength passively ML EDF laser without an intracavity modulator for the first time, to the best of our knowledge. Utilizing the emission re-absorption of the EDF, the gain at the 1530 nm region is gradually suppressed as the length of the EDF increases. With a proper length of EDF, the gain intensities of the 1530 nm region and 1550 nm region are very close. The dual-wavelength pulse can be realized easily with a 0.3 m EDF as the gain fiber and intracavity dispersion of  $-0.0761 \text{ ps}^2$ . Two spectral peaks with close intensities are located at 1532 and 1552 nm, respectively. The maximum output power is 4.7 mW at a repetition rate of 57.65 MHz. The self-starting simple structured dual-wavelength ML EDF laser can meet many potential applications.

This work was supported by the National Natural Science Foundation of China (NSFC) (Nos. 61475162 and 61377103), the Key Project of Bureau of International Co-operation, Chinese Academy of Sciences (No. 181811KYSB20160029), and the Key Research Project of Bureau of Frontier Sciences and Education, Chinese Academy of Sciences (No. QYZDY-SSW-JSC008).

## References

1. X. Zhao, Z. Zheng, L. Liu, Y. Liu, Y. Jiang, X. Yang, and J. Zhu, *Opt. Express* **19**, 1168 (2011).

2. S. Huang, Y. Wang, P. Yan, J. Zhao, H. Li, and R. Lin, *Opt. Express* **22**, 11417 (2015).
3. J. Zhou, A. Luo, Z. Luo, X. Wang, X. Feng, and B. Guan, *Photon. Res.* **3**, A21 (2015).
4. S. J. Tan, H. Haris, and S. W. Harun, *Chin. Opt. Lett.* **15**, 101401 (2017).
5. S. Li, K. Chan, Y. Liu, L. Zhang, and I. Bennion, *IEEE Photon. Technol. Lett.* **10**, 1712 (1998).
6. G. Lin, H. Wang, G. Lin, Y. Huang, Y. Lin, and T. Cheng, *J. Lightwave Technol.* **27**, 552 (2009).
7. G. Lin, T. Cheng, Y. Chi, G. Lin, H. Wang, and Y. Lin, *Opt. Express* **17**, 17739 (2009).
8. G. Lin, Y. Liao, Y. Chi, H. Kuo, G. Lin, H. Wang, and Y. Chen, *J. Lightwave Technol.* **28**, 2925 (2010).
9. M. Zhang, D. Wang, H. Li, and W. Jin, *IEEE Photon. Technol. Lett.* **14**, 92 (2002).
10. Z. Zhang and T. Yagi, *Opt. Lett.* **18**, 2126 (1993).
11. C. Zhu, J. He, and S. Wang, *Opt. Lett.* **30**, 561 (2005).
12. G. Xie, D. Tang, H. Luo, H. Zhang, H. Yu, J. Wang, X. Tao, M. Jiang, and L. Qian, *Opt. Lett.* **33**, 1872 (2008).
13. H. Yoshioka, S. Nakamura, T. Ogawa, and S. Wada, *Opt. Express* **18**, 1479 (2010).
14. J. B. Schlager, S. Kawanishi, and M. Saruwatari, *Electron. Lett.* **27**, 2072 (1991).
15. G. E. Town, L. Chen, and P. W. E. Smith, *IEEE Photon. Technol. Lett.* **12**, 1459 (2000).
16. H. Dong, G. H. Zhu, Q. Wang, H. Z. Sun, and N. K. Dutta, *Opt. Express* **12**, 4297 (2004).
17. J. Yao, J. Yao, Y. Wang, S. C. Tjin, Y. Zhou, Y. L. Lam, J. Liu, and C. Lu, *Opt. Commun.* **191**, 341 (2001).
18. Z. Chen, H. Sun, S. Ma, and N. K. Dutta, *IEEE Photon. Technol. Lett.* **20**, 2066 (2008).
19. S. Pan and C. Lou, *IEEE Photon. Technol. Lett.* **18**, 1451 (2006).
20. A. Jain, N. Chandra, A. Anchal, and K. K. Pradeep, *Opt. Laser Technol.* **83**, 189 (2016).
21. D. Mao and H. Lu, *J. Opt. Soc. Am. B* **29**, 2819 (2012).
22. A. Luo, Z. Luo, W. Xu, V. V. Dvovrin, V. M. Mashinsky, and E. M. Dianov, *Laser Phys. Lett.* **8**, 601 (2011).
23. Z. C. Tiu, S. J. Tan, H. Ahmad, and S. W. Harun, *Chin. Opt. Lett.* **12**, 113202 (2014).
24. Z. Wang, S. Du, J. Wang, F. Zou, Z. Wang, W. Wu, and J. Zhou, *Chin. Opt. Lett.* **14**, 041401 (2016).
25. X. Jin, X. Wang, X. Wang, and P. Zhou, *Appl. Opt.* **54**, 8260 (2015).
26. L. Yun, X. Liu, and D. Mao, *Opt. Express* **20**, 20992 (2012).
27. H. Zhang, D. Tang, X. Wu, and L. Zhao, *Opt. Express* **17**, 12692 (2009).
28. Z. Luo, A. Luo, and W. Xu, *IEEE Photon. J.* **3**, 64 (2011).
29. Z. Zhang, Z. Xu, and L. Zhang, *Opt. Express* **20**, 26736 (2012).
30. Z. Luo, J. Wang, M. Zhou, H. Xu, Z. Cai, and C. Ye, *Laser Phys. Lett.* **9**, 229 (2012).
31. M. Liu, N. Zhao, H. Liu, X. Zheng, A. Luo, Z. Luo, W. Xu, C. Zhao, H. Zhang, and S. Wen, *IEEE Photon. Technol. Lett.* **26**, 983 (2014).
32. B. Guo, Y. Yao, J. Xiao, R. Wang, and J. Zhang, *IEEE J. Sel. Top. Quantum Electron.* **22**, 0900108 (2016).
33. C. Zeng, Y. Cui, and J. Guo, *Opt. Commun.* **347**, 44 (2015).
34. A. Komarov, H. Leblond, and F. Sanchez, *Phys. Rev. A* **71**, 053809 (2005).
35. E. Desurvire and J. R. Simpson, *J. Lightwave Technol.* **7**, 835 (1989).
36. G. P. Agrawal, *Nonlinear Fiber Optics*, 4th ed. (Academic, 2007).